Acta Crystallographica Section D
Biological Crystallography
ISSN 0907-4449

Crystallization and X-ray diffraction data of a tRNA^{Sec} acceptor-stem helix

Charlotte Förster,[a] Andrea Eickmann,[a] Uwe Schubert,[a] Susanne Hollmann,[a] Uwe Müller,[b] Udo Heinemann[b,c] and Jens Peter Fürste[a]*†

[a]Freie Universität Berlin, Institüt für Biochemie, Thielallee 63, 14195 Berlin, Germany, [b]Forschungsgruppe Kristallographie, Max-Delbrück-Centrum für Molekulare Medizin, Robert-Rössle-Strasse 10, 13122 Berlin, Germany, and [c]Freie Universität Berlin, Institüt für Kristallographie, Takustrasse 6, 14195 Berlin, Germany

† Present address: NOXXON Pharma AG, Gustav-Meyer-Allee 25, 13355 Berlin, Germany.

Correspondence e-mail: jfuerste@noxxon.net

Received 12 January 1998
Accepted 18 May 1998

tRNA^{Sec} is a UGA suppressor tRNA which co-translationally inserts selenocysteine into proteins. Its eight-base-pair tRNA^{Sec} acceptor stem, which contains key recognition elements, was synthesized using solid-phase phosphoramidite RNA chemistry. High-resolution X-ray diffraction data were collected using synchrotron radiation under cryogenic cooling conditions. The crystals diffract to a maximal resolution of 1.8 Å. X-ray diffraction data were processed to 2.4 Å. tRNA^{Sec} microhelix crystallizes in space group $R32$, with cell constants a = 47.02, b = 47.02, c = 373.03 Å, $\alpha = \beta = 90$, $\gamma = 120^\circ$. The crystals contain three RNA molecules per asymmetric unit.

1. Introduction

Selenocysteine is referred to as the '21st amino acid' in *in vivo* protein biosynthesis. Selenocysteinyl-tRNA^{Sec} inserts this amino acid into proteins by a suppression mechanism at certain UGA stop codons which are located in a defined mRNA context (Zinoni *et al.*, 1987; Leinfelder *et al.*, 1988; Thormay *et al.*, 1994). tRNA^{Sec} is first aminoacylated with serine by seryl-tRNA synthetase. Seryl-tRNA^{Sec} is converted to selenocysteinyl-tRNA^{Sec} (Sec-tRNA^{Sec}) by selenocysteine synthase, an enzyme which replaces the hydroxyl group of the tRNA-bound seryl residue by a selenol group (Forchhammer, Boesmiller *et al.*, 1991; Forchhammer, Leinfelder *et al.*, 1991; Forchhammer & Böck, 1991). Sec-tRNA^{Sec} binds to elongation factor SELB (Forchhammer *et al.*, 1989, 1990; Forchhammer, Boesmiller *et al.*, 1991; Forchhammer, Leinfelder *et al.*, 1991). This protein directs the incorporation of selenocysteine at UGA codons by Sec-tRNA^{Sec} suppression. The interaction between a defined stem-loop region at the mRNA 3′ end and the SELB–Sec-tRNA^{Sec} complex allows the suppression of the UGA codon at the A site of the ribosome and the co-translational insertion of selenocysteine into the polypeptide chain.

Selenocysteinyl-tRNA^{Sec} has no binding affinity for the canonical elongation factor EF-Tu (Förster *et al.*, 1990) but binds its own factor with analogous function, SELB. The determinants in tRNA^{Sec} which discriminate between EF-Tu and SELB binding are located on the aminoacyl stem of the RNA molecule and are therefore responsible for tRNA^{Sec} identity. First, tRNA^{Sec} possesses an eight-base-pair acceptor stem instead of the seven-base-pair stem in elongator tRNAs (Baron & Böck, 1991). Second, certain sequence motifs and identity elements play a role in determination of tRNA^{Sec} identity (Rudinger *et al.*, 1996).

We wish to investigate a high-resolution X-ray structure of the tRNA^{Sec} aminoacyl stem in order to compare its structure to the two related serine-specific acceptor-stem helices which were recently crystallized (Förster *et al.*, unpublished work) and their structures solved to atomic resolution (Müller *et al.*, 1999). High-resolution structures of serine and selenocysteine tRNA microhelices will help in the understanding of the molecular and structural discrimination between elongation of ribosomal protein biosynthesis and suppression by Sec-tRNA^{Sec}. Also, we hope to contribute to the understanding of tRNA–aminoacyl-tRNA-synthetase interaction demonstrated by the serine and selenocysteine system.

2. Materials and methods

2.1. RNA synthesis and purification

Both strands of tRNA^{Sec} microhelix were synthesized using automated solid-phase phosphoramidite RNA chemistry. Synthesis was performed on an Applied Biosystems synthesizer with the following Chemgenes RNA phosphoramidites (Waltham, MA, USA): 5′-DMT-2′-tBD silyl-ribo adenosine (*N*-benzoyl) CED phosphoramidite, 5′-DMT-2′-tBD silyl-ribo cytidine (*N*-benzoyl) CED phosphoramidite, 5′-DMT-2′-tBD silyl-ribo guanosine (*N*-isobutyl) CED phosphoramidite and 5′-DMT-2′-tBD silyl-ribo uridine CED phosphoramidite. 0.15 µmol of each amidite was dissolved in water-free acetonitrile. Synthesis was performed on a 1 µmol (64 step cycle) CPG 500 Å Chemgenes column (Waltham, MA, USA). Deprotection took place in 48 h at 310 K in 1 ml moisture-free

Table 1
Crystallographic and X-ray diffraction data for $tRNA^{Sec}$ acceptor-stem helix (SEC).

Crystal size (mm)	0.2 × 0.1 × 0.1
Cell axes (Å)	a = 47.02, b = 47.02, c = 373.03
Cell angles (°)	α = 90, β = 90, γ = 120
Space group	$R32$
Volume of the unit cell ($Å^3$)	714209
Molecular weight of the RNA helix (Da)	5019
V_M ($Å^3$ Da^{-1})	2.64
RNA duplexes per asymmetic unit	3
Radiation source	Synchotron
Wavelength (Å)	1.000
Detector	180 mm IP
Temperature (K)	100
Maximal resolution (Å)	1.8
Resolution range (Å)	39.8–2.4
Measurements	85053
Unique reflections	6716
Completeness (%)	100
R_{merge} (%)	10.8
R_{sym} (last resolution shell) (%)	38.5
Completeness (last resolution shell) (%)	100

ethanolic ammonia. After taking an aliquot for determination of the UV absorption, both RNA strands were lyophilized. 10 µl 98% triethylamine hydrofluoride were added per A_{260} RNA and incubated for 72 h at room temperature. After addition of 2 µl H_2O and 100 µl 1-butanol per A_{260} RNA at 253 K overnight and centrifugation at 13000 rev min^{-1}, all pellets were redissolved in H_2O. The yield of RNA was determined by UV absorption (Sproat *et al.*, 1995)

For crystallization, RNA strands were purified by reversed-phase HPLC on an RP 18 column. Elution of RNA oligonucleotides took place using a linear gradient of 1–15% buffer *B* in buffer *A* at a flow rate of 1 ml min^{-1} at 318 K, where buffer *A* consists of 100 m*M* triethyl ammonium acetate (Millipore water) pH 8.0 and buffer *B* is 100 m*M* triethyl ammonium acetate pH 7.5 in 80% acetonitrile. The purified RNA oligonucleotides were lyophilized, resuspended in Millipore water and the yield determined by UV absorption.

2.2. RNA hybridization and crystallization

The purified eight-base-pair complementary RNA strands were hybridized in water at a concentration of 0.5 m*M* at 355 K and slowly cooled to room temperature within several hours to yield a $tRNA^{Sec}$ acceptor-stem duplex. Crystallization experiments were performed using the hanging-drop vapour-diffusion technique at 291 K. Very small crystals (dimensions smaller than 0.05 mm) were achieved using the following conditions: 1 µl of 0.5 m*M* $tRNA^{Sec}$ acceptor-stem duplex (SEC) added to 1 µl of 40 m*M* cacodylate pH 7.0, 12 m*M* spermine tetrachloride, 40 m*M* lithium chloride, 80 m*M* strontium chloride and 10%(*v*/*v*) methyl pentanediol equilibrated against 1 ml 40%(*v*/*v*) methyl pentanediol reservoir solution.

Crystallization conditions could be improved to yield crystals with dimensions 0.2 × 0.1 × 0.1 mm by addition of 1 µl 0.5 m*M* SEC to 1 µl 40 m*M* cacodylate pH 7.0, 12 m*M* spermine tetrachloride, 80 m*M* sodium chloride, 12 m*M* potassium chloride, 20 m*M* magnesium chloride and 10%(*v*/*v*) methyl pentanediol equilibrated against 1 ml 40%(*v*/*v*) methyl pentanediol.

2.3. Crystallographic data collection and evaluation

X-ray diffraction data were recorded at the Trieste synchrotron station ELETTRA, X-ray diffraction beamline 5.2R at 100 K with frozen crystals under cryogenic cooling conditions at a wavelength of λ = 1.000 Å. Data were detected on a MAR Research 180 mm imaging-plate system. Two data sets were collected: high-resolution X-ray diffraction data were collected in the resolution range 20.0–1.7 A and a low-resolution data set was collected in the range 40.0–3.0 Å. Data processing, determination of space groups and unit-cell parameters were performed with the programs *DENZO* and *SCALEPACK* (Otwinowski, 1993).

3. Results and discussion

3.1. Crystallization

The eight-base-pair sequence of the chemically synthesized $tRNA^{Sec}$ acceptor-stem helix is shown in Fig. 1. Crystals appeared within 14 and 21 d at 291 K. The dimensions of the largest crystals are 0.2 × 0.1 × 0.1 mm. They show a rhombohedral morphology with angles α = 90, β = 90, γ = 120°, as can be seen in Fig. 2.

SEC

5′ G–C 3′
G–C
A–U
A–U
G–C
A–U
U–A
C–G

Figure 1
Sequence of the eight-base-pair $tRNA^{Sec}$ acceptor-stem duplex (SEC; Steinberg *et al.*, 1993).

3.2. Crystallographic and X-ray diffraction data

$tRNA^{Sec}$ microhelix crystallizes in the rhombohedral space group *R*32. The space group can be clearly correlated to the crystal morphology of the $tRNA^{Sec}$ microhelix. Crystallographic data are given in Table 1. With a molecular weight of 5019, and assuming three RNA duplexes per asymmetric unit, the V_M value according to Matthews (1968) can be calculated to be 2.64 $Å^3$ Da^{-1} (Table 1). Portman *et al.* (1995) have recently published the X-ray structure of an eight-base-pair RNA duplex which, in addition to a hexagonal form, also crystallizes in this rhombohedral space group. This space group could be a general feature for octamer RNA-duplex crystallization.

The maximal resolution for the $tRNA^{Sec}$ microhelix crystal was 1.8 Å. Data in the

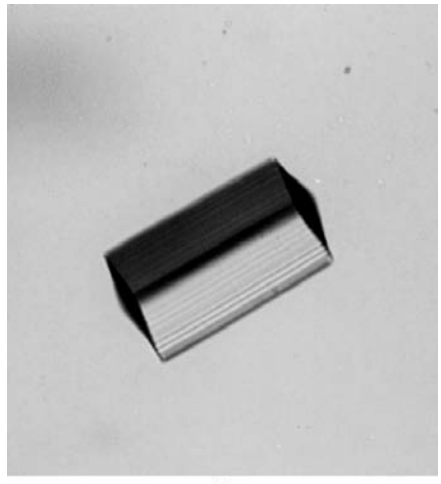

(*a*)

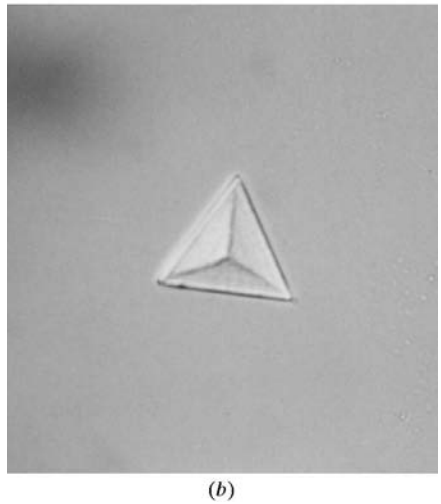

(*b*)

Figure 2
Crystals of $tRNA^{Sec}$ acceptor-stem helix show a rhombohedral morphology, which can be correlated to the space group *R*32. The size of the crystals is 0.2 × 0.1 × 0.1 mm. Photographs were taken from two different crystal orientations.

resolution range 39.8–2.4 Å were processed after merging the high-resolution and low-resolution data sets. All X-ray diffraction data are listed in Table 1. The overall $R_{\rm merge}$ is 10.8% (Table 1; $R_{\rm merge} = \sum |I_{ij} - \langle I_i \rangle| / \sum I_{ij}$, where I_{ij} are the measurements contributing to the mean reflection intensity, $\langle I_i \rangle$). Crystallization time, space group, unit cell and resolution of X-ray diffraction data differ clearly from the two seven-base-pair serine-specific tRNA microhelix crystals (Förster *et al.*, unpublished work). We believe this can be explained by the different length of the seven- and eight-base-pair RNA helices which can be compared with other crystallized RNA oligonucleotides with these lengths (Ott *et al.*, 1996; Portman *et al.*, 1995).

By solving the X-ray structure of the $tRNA^{Sec}$ microhelix, we wish to contribute to the understanding of the SELB–$Sec\text{-}RNA^{Sec}$ interaction and the rejection of this tRNA by EF-Tu. Structural investigations of the $tRNA^{Sec}$ acceptor stem may help to obtain information about the special structural elements of this RNA and therefore contribute to the understanding of co-translational selenocysteine incorporation.

We thank Dr V. A. Erdmann for support and discussions. Assistance during measurements at the Trieste synchrotron ELETTRA was provided by Edoardo Busetto and Luca Olivi. This work was supported by SFB 344, DFG He 1318/13-2 and Fonds der Chemischen Industrie.

References

Baron, C. & Böck, A. (1991). *J. Biol. Chem.* **266**, 20375–20379.
Forchhammer, K. & Böck, A. (1991). *J. Biol. Chem.* **266**, 6324–6328.
Forchhammer, K., Boesmiller, K. & Böck, A. (1991). *Biochimie*, **73**, 1481–1486.
Forchhammer, K., Leinfelder, W. & Böck, A. (1989). *Nature (London)*, **342**, 453–456.
Forchhammer, K., Leinfelder, W., Boesmiller, K., Veprek, B. & Böck, A. (1991). *J. Biol. Chem.* **266**, 6318–6323.
Forchhammer, K., Rucknagel, K. P. & Böck, A. (1990). *J. Biol. Chem.* **265**, 9346–9350.
Förster, C., Ott, G., Forchhammer, K. & Sprinzl, M. (1990). *Nucleic Acids Res.* **18**, 487–491.
Leinfelder, W., Zehelein, E., Mandrand-Berthelot, M. A. & Böck, A. (1988). *Nature (London)*, **331**, 723–725.
Matthews, B. W. (1968). *J. Mol. Biol.* **33**, 491–497.
Müller, U., Förster, C., Fürste, J. P. & Heinemann, U. (1999). In preparation.
Ott, G., Dörfler, S., Sprinzl, M., Müller, U., & Heinemann, U. (1996). *Acta Cryst.* D**52**, 871–873.
Otwinowski, Z. (1993). *DENZO. An Oscillation Data Processing Program for Macromolecular Crystallography.* Yale University, New Haven, CT, USA.
Portman, S., Usman, N. & Egli, M. (1995). *Biochemistry*, **34**, 7569–7575.
Rudinger, J., Hillenbrandt, R., Sprinzl, M. & Giegé, R. (1996). *EMBO J.* **15**, 650–657.
Sproat, B., Colonna, F., Mullah, B., Tsou, D., Andrus, A., Hampel, A. & Vinayak, R. (1995). *Nucleosides Nucleotides*, **14**, 255–273.
Steinberg, S., Misch, A. & Sprinzl, M. (1993). *Nucleic Acids Res.* **21**, 3011–3015.
Thormay, P., Wilting, R., Heider, J. & Böck, A. (1994). *J. Bacteriol.* **176**, 1268–1274.
Zinoni, F., Birkmann, A., Leinfelder, W. & Böck, A. (1987). *Proc. Natl Acad. Sci. USA*, **84**, 3156–3160.